

Acoustoconductance in a nonuniform quantum channel

H. Totland and Ø. L. Bø

Department of Physics, University of Oslo, P.O. Box 1048 Blindern, N-0316 Oslo, Norway

Y. M. Galperin

Department of Physics, University of Oslo, P.O. Box 1048 Blindern, N-0316 Oslo, Norway

and A. F. Ioffe Physico-Technical Institute, 194021 St. Petersburg, Russia

(Received 7 May 1997)

We consider the influence of a surface acoustic wave on the conductance through a ballistic quantum channel with an adiabatic geometry produced by split gates in a two-dimensional electron gas. The surface acoustic wave leads to a contribution to the conductance of the quantum channel. This contribution, called the acoustoconductance, is shown to oscillate as a function of the Fermi level, which is controlled by the gate voltage. [S0163-1829(97)01348-9]

I. INTRODUCTION

A quantum point contact (QPC), or quantum channel, is a narrow constriction that separates two regions of large conductivity. It can be produced in a two-dimensional electron gas (2DEG) by means of a split gate at negative voltage. In such a configuration, the geometrical parameters of the channel can be tuned by the gate voltage. Under proper conditions (see, e.g., Ref. 1 and references therein), the electron motion in the transverse direction is quantized, and each electron state is characterized by three quantum numbers: its energy E , a mode number n describing transverse motion, and the direction of propagation (\pm).

The conductance G^0 of a ballistic QPC is known to be a steplike function of the gate voltage.¹⁻³ This is described by the Landauer formula,⁴ which relates the conductance to the number of occupied modes, each mode contributing a quantum $2e^2/h$ of conductance multiplied by a transmission probability (typically close to either 0 or 1).

The interaction of electrons in a QPC with external fields, as well as with dynamical degrees of freedom of the surrounding, is the focus of interest of many research groups. In this connection, several sources of influence on the QPC conductance have been studied. In particular, the non-Ohmic behavior of the conductance due to interaction with equilibrium phonons has been extensively studied, starting from Refs. 5 and 6.

Another source of influence that leads to transitions between different modes and thus affects the Ohmic conductance is that of a high-frequency transverse electric field. In Ref. 7, the microwave-induced contribution, called the photoconductance G^{ph} , was calculated for an adiabatically smooth QPC and a small bias voltage. As a function of the gate voltage, G^{ph} shows steplike oscillations.

Much attention has been attracted by the various effects that can result from the interaction between a 2DEG and nonequilibrium acoustical phonons, both incoherent⁸⁻¹⁴ and coherent.¹⁵⁻²⁸ In the latter case, which is relevant to this paper, a surface acoustic wave (SAW) is induced in a piezoelectric substrate, on top of which the low-dimensional struc-

ture is mounted. While propagating, the SAW generates a traveling electric field wave that acts upon the electrons. That results, in particular, in the attenuation and change of velocity of the wave, the effects being *linear* in the wave's amplitude at small amplitudes.¹⁵⁻²¹ In mesoscopic systems, however, the detection and measurement of such effects are difficult because of the small sizes of mesoscopic devices.

Better suited for detection are the influences of the SAW on *dc electric properties* of a QPC. These are the *acoustoelectric effect*²²⁻²⁸ and the *acoustoconductance*. The first effect means the drag of 2D electrons by a SAW, creating a dc acoustoelectric current (or, in an open circuit, an acoustoelectric voltage). The second one is the variation of the dc conductance of the QPC due to the SAW. Both effects are *nonlinear* in the amplitude—at low intensities, they are proportional to the *intensity* of the wave.

Recently, the acoustoelectric current through a uniform quantum channel has been studied, both experimentally²⁷ and theoretically.^{27,29} Contrary to the steplike behavior that might have been expected, the current showed giant oscillations (cf. with Ref. 30) as a function of the gate voltage, the minima coinciding with the conductance plateaus. This oscillatory behavior has been explained by the interaction between the SAW and the electrons inside the quantum channel. The maxima correspond to Fermi level positions where the upper mode Fermi velocity is close to the wave velocity, s , thus resulting in a strong interaction. The acoustoelectric effect in a long, uniform channel was also theoretically considered in Ref. 31; effects on the acoustoelectric current due to the edges of a nonuniform QPC were studied theoretically in Ref. 32.

At sufficiently high SAW intensities,²⁸ an acoustoelectric current has been found to be present even in a region of gate voltages below the pinch-off value. In this region, the current, starting from zero, makes (a few) steps of height $\Delta I = ef$ with increasing gate voltage, $f = \omega/2\pi$ being the frequency of the wave. Within each plateau region, this corresponds to a picture in which each minimum of the traveling wave potential carries the same (integer) number of elec-

trons. Furthermore, as the SAW intensity is varied within a certain range, the height of each plateau remains the same, only its position along the gate voltage axis is shifted. Such a universal behavior needs more theoretical effort to be understood.

Exposing a QPC to the influence of both a low-intensity SAW and a small bias voltage V will lead to a dc current $I = I^{\text{ac}} + GV$, where I^{ac} is the acoustoelectric current at $V = 0$, and G is the (Ohmic) conductance in the presence of the SAW. Both of these quantities depend on the Fermi level, and, consequently, on the gate voltage. G is the sum of the zero field conductance G^0 discussed above and a correction term G^{ac} , called the acoustoconductance. To lowest orders, G^{ac} should be proportional to the SAW intensity (while constant in V).

The aim of this paper is to study theoretically the acoustoconductance in a long enough, adiabatic (i.e., with a smoothly varying width) quantum point contact formed in a 2DEG by a split gate. ‘‘Long enough’’ means that the channel’s length l is much greater than the SAW wavelength $2\pi/q$. To our knowledge, no measurements of the acoustoconductance in such a situation have been made so far.

In contrast to the present paper, the main subject of Refs. 29 and 32 is the SAW-induced contribution to the electric current. In Ref. 29, a uniform channel is considered. Reference 32 deals with a nonuniform channel, presenting a qualitative description of the edge effects as well as numerical calculations. Similar edge effects are at play in the situation considered here. Below we obtain a semiquantitative formula for the acoustoconductance.

The paper is organized as follows. In Sec. II, the approximations relevant to the present problem, namely, the adiabatic and the stationary phase approximations, are briefly discussed. These are then employed in Sec. III to find the dependence of the acoustoconductance on the Fermi energy. In the last section, the resulting formula is discussed and plotted for a specific channel geometry and given parameters.

II. FORMULATION OF THE PROBLEM

In the adiabatic approximation (cf., for example, Ref. 33), the electron wave function for a propagating state can be written as

$$|n, p\rangle = \chi_{n,x}(y) \sqrt{\frac{|p|}{|p(x)|L}} \exp\left(\frac{i}{\hbar} \int^x p(x') dx'\right).$$

In this expression, the transverse wave functions χ_n as well as the corresponding eigenvalues E_n are assumed to vary slowly with the longitudinal coordinate x . The longitudinal momentum is defined as $p(x) = \pm \sqrt{2m[E - E_n(x)]}$, $E > \max\{E_n(x)\}$, while $|p|$ denotes $|p(\pm\infty)| \equiv \sqrt{2mE}$, m being the effective mass. The normalization length L is large compared to the channel’s length and will not appear in the final formulas. The above assumption means that for each mode, one is effectively dealing with the one-dimensional motion of electrons in a smooth potential $E_n(x)$, which is determined by the x -dependent confinement in the y direction provided by the split gate. For a reflecting state, $E < \max\{E_n(x)\}$, the wave function is given by

$$|n, p\rangle = \chi_{n,x}(y) \sqrt{\frac{2|p|}{|p(x)|L}} \sin\left(\frac{1}{\hbar} \int_{x_t}^x p(x') dx'\right),$$

x_t being the classical turning point. In this case one has to discriminate between the states on the left-hand side (lhs) and on the rhs of the channel.

We consider the case of a SAW propagating in the longitudinal direction. The induced electric field will propagate and be polarized in the x direction (see Ref. 34 for more details). Thus one can allow for the influence of the SAW by calculating the SAW-induced scattering due to perturbation through a potential $V(x, y, t) = V_0(x, y) \cos(qx - \omega t)$. The envelope function $V_0(x, y)$ is determined by the screening of the piezoelectric field by the electrons inside the leads and the channel. The screening in the 2D leads is very strong because of the high conductance of the 2DEG. However, if the channel is narrow enough in comparison with the effective Bohr radius $\epsilon\hbar^2/me^2$, then the screening inside the channel is weak and the effective potential V_0 is of the order of the unscreened one (cf. with Ref. 35). As a result, in a narrow channel and at

$$ql \gg 1, \quad (1)$$

where l is the effective length of the channel, one can consider the function $V_0(x, y)$ as a smooth function $V_0(x)$ inside the channel and rapidly decreasing outside. Consequently, there are no acoustically induced intermode transitions, and we can thus treat each mode separately with a perturbing field $V_0(x) \cos(qx - \omega t)$.

Another simplification which arises from the inequality (1) is that one can employ the *stationary phase approximation* to estimate the corresponding transition probability. In this approximation, a typical transition amplitude

$$\langle n, p_2 | V | n, p_1 \rangle = \int_{-\infty}^{\infty} dx A(x) e^{i\varphi(x)} \quad (2)$$

is approximated by expanding its integrand’s phase

$$\varphi(x) = \pm qx + \hbar^{-1} \int^x [p_1(x') - p_2(x')] dx'$$

around a stationary point x^* defined by the equation $d\varphi/dx = 0$,^{36,37}

$$\varphi(x) = \varphi(x^*) + \frac{1}{2} \varphi''(x^*) (x - x^*)^2. \quad (3)$$

If φ has no stationary points, one assumes a rapidly oscillating phase everywhere, whence the total contribution to the transition amplitude almost cancels. In this picture, the transitions are localized to points x^* where $\varphi'(x^*) = 0$, and one can substitute $A(x)$ in the integrand by $A(x^*)$. In our case, the change in energy $+\hbar\omega$ due to absorption of the (SAW) phonon is accompanied by a momentum transfer $+\hbar q$, i.e., at the point of stationary phase one arrives at the *local* conservation condition,

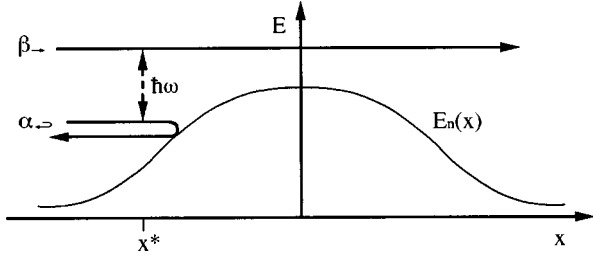


FIG. 1. SAW-induced transition between a reflecting and a propagating state.

$$\sqrt{2m[E + \hbar\omega - E_n(x^*)]} = \pm \sqrt{2m[E - E_n(x^*)]} + \hbar q.$$

The above approach was effectively employed in Ref. 7 to analyze the photoconductance. However, the photoconductance case differs from the present situation in two aspects. First, there is no momentum transfer to the electrons from an oscillating transverse electric field ($q \approx 0$). Consequently, in a symmetric QPC, the net current is still zero at $V=0$. [In the stationary phase approximation, the momentum $p(x^*)$ is conserved at a transition.] Secondly, the y polarization of the field causes intermode transitions. This leads to a mechanism of indirect forward and backscattering, the transitions taking place between the propagating states of mode number n and the nonpropagating states with a different mode number m . When $V \neq 0$, these processes have a net effect on the current; that is, the conductance acquires a correction term G^{ph} , called the photoconductance.

III. CALCULATION OF THE ACOUSTOCONDUCTANCE

To find a formula for the acoustoconductance, we start by noticing that, in the stationary phase approximation, there are only two possible kinds of SAW-induced (intramode) transitions that change the net current: (i) transitions between re-

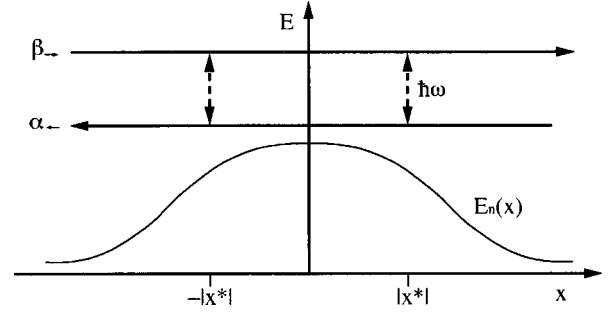


FIG. 2. SAW-induced transition between two oppositely directed propagating states.

flecting states $|\alpha_{\leftarrow}\rangle$ on the lhs and right-moving, propagating states $|\beta_{\leftarrow}\rangle$ (cf. Fig. 1), and (ii) transitions between left-moving, propagating states $|\alpha_{\leftarrow}\rangle$ and right-moving, propagating states $|\beta_{\leftarrow}\rangle$ (cf. Fig. 2). Here the energy and momentum differences between the states β and α are $\hbar\omega$ and $\hbar q$, respectively.

The current through the QPC can be expressed in terms of the corresponding transition rates $w(\beta, \alpha)$ (determined by the Fermi golden rule for the transition $\alpha \rightarrow \beta$) and the occupation numbers $f_{\alpha(\beta)}$. For a small bias voltage V , the Fermi function is

$$f_{\alpha} = f_{\alpha}^0 \left(\mu \pm \frac{eV}{2} \right) = f_{\alpha}^0 \pm \frac{eV}{2} \frac{\partial f_{\alpha}^0}{\partial \mu}, \quad (4)$$

with $f_{\alpha}^0 = [e^{(E_{\alpha} - \mu)/k_B T} + 1]^{-1}$. In Eq. (4), the $+$ sign is taken for electrons originating on the lhs of the QPC (α_{\leftarrow} and α_{\rightarrow}), the $-$ sign for those originating on the rhs (α_{\leftarrow}). The total SAW-induced current, i.e., the total current minus the zero-field Ohmic part $G^0 V$, is (including spin) given by the expression

$$I_{\text{tot}}^{\text{ac}} \equiv I^{\text{ac}} + G^{\text{ac}} V = 2e \sum_{\alpha\beta} [w(\beta_{\rightarrow}, \alpha_{\leftarrow}) + w(\beta_{\leftarrow}, \alpha_{\rightarrow}) - w(\beta_{\leftarrow}, \alpha_{\leftarrow}) - w(\beta_{\rightarrow}, \alpha_{\rightarrow})] f_{\alpha} \quad (5)$$

$$= \frac{\pi e}{\hbar} \sum_{\alpha\beta} \left\{ [|\langle \beta_{\rightarrow} | V_0(x) e^{iqx} | \alpha_{\leftarrow} \rangle|^2 + |\langle \beta_{\leftarrow} | V_0(x) e^{iqx} | \alpha_{\rightarrow} \rangle|^2] \delta(E_{\beta} - E_{\alpha} - \hbar\omega) - [|\langle \beta_{\leftarrow} | V_0(x) e^{-iqx} | \alpha_{\leftarrow} \rangle|^2 + |\langle \beta_{\rightarrow} | V_0(x) e^{-iqx} | \alpha_{\rightarrow} \rangle|^2] \delta(E_{\alpha} - E_{\beta} - \hbar\omega) \right\} f_{\alpha}. \quad (6)$$

(The arrows express the conditions of, respectively, propagation in the indicated direction, and reflection on the lhs of the channel.) Here I^{ac} is called the *acoustoelectric* current, which is just the drag current at zero bias voltage. Equation (5) can be derived similarly to the expression for the photoconductivity.⁷ By inserting Eq. (4) into Eq. (6), the acoustoconductance G^{ac} is found to be

$$G^{\text{ac}} = \frac{\pi e^2}{2\hbar} \sum_{\alpha\beta} \frac{\partial f_{\alpha}^0}{\partial \mu} \left\{ [|\langle \beta_{\rightarrow} | V_0(x) e^{iqx} | \alpha_{\leftarrow} \rangle|^2 - |\langle \beta_{\leftarrow} | V_0(x) e^{iqx} | \alpha_{\rightarrow} \rangle|^2] \delta(E_{\beta} - E_{\alpha} - \hbar\omega) + [-|\langle \alpha_{\leftarrow} | V_0(x) e^{iqx} | \beta_{\leftarrow} \rangle|^2 - |\langle \alpha_{\rightarrow} | V_0(x) e^{iqx} | \beta_{\rightarrow} \rangle|^2] \delta(E_{\alpha} - E_{\beta} - \hbar\omega) \right\}. \quad (7)$$

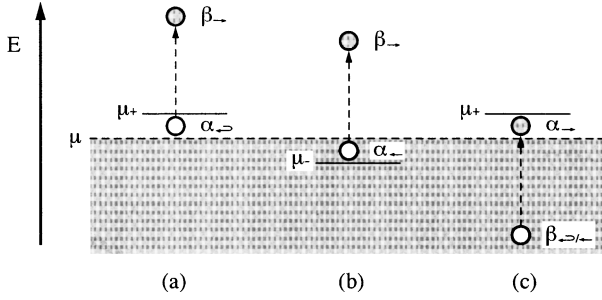


FIG. 3. As the bias voltage V is turned on, the increased local Fermi level $\mu_+ = \mu + eV/2$ on the lhs of the QPC allows for additional processes of the kind shown in (a), but fewer ones of the kind (c), while the decreased local Fermi level $\mu_- = \mu - eV/2$ on the rhs suppresses the kind of process shown in (b). As a result, there are one positive and three negative terms in the formula for the acoustoconductance.

The signs in front of the four terms in the sum in Eq. (7) can be explained as follows. Suppose a small bias voltage V is applied. Then the (quasi) Fermi level goes up on the lhs of the channel and down on the rhs. Consequently, new states α_- get occupied on the lhs, which means that more transitions of the kind $\alpha_- \rightarrow \beta_-$ become possible [Fig. 3(a)]. The result is an *increased* particle current, and, consequently, a positive contribution to the conductance described by the first term. At the same time, the number of occupied states α_- on the rhs becomes smaller, and thus, as expressed in the second term in Eq. (7), the particle current *decreases* [Fig. 3(b)]. Similarly, transitions *to* states α_- just above the original Fermi level are no longer possible, because the increased Fermi level on the lhs means that these states are already occupied [Fig. 3(c)]. Thus there will be *fewer* transitions of the kind $\beta_- \rightarrow \alpha_-$, corresponding to the last two terms.

Inserting the normalized wave functions, one can express the first transition amplitude as

$$\langle \beta_- | V_0(x) e^{iqx} | \alpha_- \rangle = \pm \delta_{nm} \frac{\sqrt{|p_\alpha p_\beta|}}{\sqrt{2} iL} \int \frac{dx V_0(x) e^{i\varphi(x)}}{\sqrt{|p_\alpha(x) p_\beta(x)|}},$$

keeping only one part of the integral.³⁷ In the stationary phase approximation, the integral is replaced by

$$V_0(x^*) \left(\frac{2\pi}{|p_\alpha(x^*) p_\beta(x^*) \varphi''(x^*)|} \right)^{1/2} \times e^{i\{\varphi(x^*) + (\pi/4) \text{sgn}[\varphi''(x^*)]\}}.$$

The momenta $p_\alpha(x^*)$ and $p_\beta(x^*)$ at the transition point are fixed by the conditions

$$\frac{p_\beta(x^*)^2}{2m} = \frac{p_\alpha(x^*)^2}{2m} \pm \hbar \omega, \quad p_\beta(x^*) = p_\alpha(x^*) \pm \hbar q.$$

The upper sign is taken here and in the case of the second transition in Eq. (7), the lower sign elsewhere. We get $p_\alpha(x^*) = p_\mp$, $p_\beta(x^*) = p_\pm$, where

$$p_\pm \equiv mw \pm \hbar q/2, \quad (8)$$

while $w = \omega/q$ is the sound velocity. If, as in the case of a parabolic or square confining potential, the transverse energy has the form $E_n(x) = \alpha_n/[d(x)]^2$, $d(x)$ being the thickness of the channel, then we have

$$\varphi''(x^*) = \frac{p'_\alpha(x^*) - p'_\beta(x^*)}{\hbar} = \frac{2mqE_n(x^*)}{p_+ p_-} \frac{d'(x^*)}{d(x^*)}.$$

The transition probability is thus proportional to

$$|\langle \beta_- | V_0(x) e^{iqx} | \alpha_- \rangle|^2 = \delta_{nm}^2 \frac{\pi V_0^2(x^*) \sqrt{E_\alpha E_\beta}}{qL^2 E_n(x^*)} \frac{d(x^*)}{|d'(x^*)|}.$$

For the second term in Eq. (7), $|\langle \beta_- | V_0(x) e^{iqx} | \alpha_- \rangle|^2$, there will be no stationary point x^* unless $p_\alpha(x^*) \equiv p_-$ is negative. Consequently, this term gives a nonzero contribution only if $\hbar q > 2mw$ (cf. Ref. 31). However, if this condition is satisfied by the wave parameters ω and q , then, as has been pointed out in Ref. 32, there will actually be *two* transition points. This results in the interference of the reflected waves, and the transition amplitude is a sum of the contributions from a ‘‘left’’ transition at $x_L^* = -|x^*|$ and a ‘‘right’’ transition at $x_R^* = +|x^*|$ (cf. Fig. 2). These two terms are calculated as the transition amplitude above; however, the factor $\sqrt{2}i$ in the denominator disappears, which is due to the difference in normalization between propagating and reflecting states. As the QPC is assumed to be symmetric, the functions p , d , E_n , and V_0 are symmetric in x , while d' , and thus φ'' , are antisymmetric; the phase φ itself is antisymmetric about $(0, \varphi(0))$. As a result, the transition probability is proportional to the one above for a single transition point, but with an additional, oscillating factor

$$2 | e^{i\{\varphi(x_L^*) + (\pi/4) \text{sgn}[\varphi''(x_L^*)]\}} + e^{i\{\varphi(x_R^*) + (\pi/4) \text{sgn}[\varphi''(x_R^*)]\}} |^2 = 4(1 + \sin[\varphi(|x^*|) - \varphi(-|x^*|)]). \quad (9)$$

The last two terms in Eq. (7) are treated the same way.

The integration (2) connected with a transition $\alpha_- \rightarrow \beta_-$ can be given a simple visualization. Figure 4 shows a sketch in the (bicentennial³⁸) complex plane of the curve

$$\gamma(t) = A(x^*) \int_{-\infty}^t e^{i\varphi(x)} dx \in \mathbf{C}$$

for a phase φ having the form shown in the inset. [As discussed above, the (symmetric) function $A(x)$ in the integrand of Eq. (2) is replaced by its value at a transition point x_L^* or x_R^* .] The starting point $\gamma(-\infty)$ lies at 0, while, in the stationary phase approximation, the end point $\gamma(\infty) = \langle \beta_- | V | \alpha_- \rangle$. That is, the transition probability is given as the square distance between the end points of the curve [to the degree that $\gamma(t)$ converges as $t \rightarrow \pm\infty$]. Obviously, the three strongly oscillating regions of the curve correspond to the regions of a rapidly varying phase $\varphi(x)$; at a given point $\gamma(t)$, the inclination $\arg[\gamma'(t)]$ of the curve is given by the phase $\varphi(t)$ (plus the constant angle $\arg[A(x^*)]$). The contribution from each of the two transi-

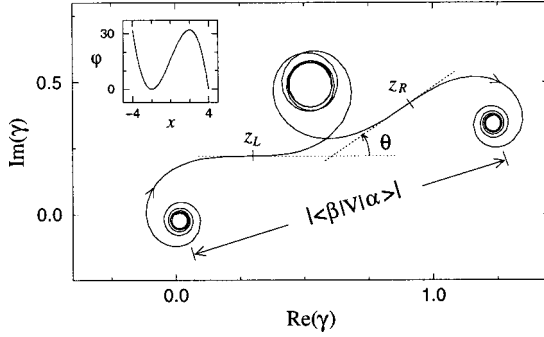


FIG. 4. Graph in the complex plane of the curve $\gamma(t) = A(x^*) \int_{-\infty}^t e^{i\varphi(x)} dx$, where $\varphi(x)$ is the function shown in the inset, and $A(x^*) = 1$ for simplicity. The oscillations are weak around the points $z_{L,R} = \gamma(x_{L,R}^*)$, corresponding to the stationary points $x_{L,R}^*$ of φ . The transition amplitude $\langle \beta_- | V | \alpha_- \rangle = \gamma(\infty) [-\gamma(-\infty)]$ depends strongly on the angle $\theta = [\varphi(x_R^*) - \varphi(x_L^*)] \bmod 2\pi$.

tion points $x_{L,R}^*$ corresponds, roughly, to the double spiral centered at $z_{L,R} = \gamma(x_{L,R}^*)$, respectively. It is the transition probability's crucial dependence on the angle $\theta = [\varphi(x_R^*) - \varphi(x_L^*)] \bmod 2\pi$ that leads to the sinusoidal factor (9). For a transition $\alpha_- \rightarrow \beta_-$, there is only one double spiral, and, consequently, no such sinusoidal factor.

In Eq. (7) we change the sum over states to an integral over energies, $\sum_{\alpha\beta} \rightarrow \int dE_\alpha dE_\beta g(E_\alpha) g(E_\beta)$, where $g(E) = L\sqrt{m/h}\sqrt{2E}$ is the density of states (for a specified direction of propagation or side of reflection). The acoustoconductance is then, finally, given by

$$G^{\text{ac}}(\mu) = \frac{e^2}{\pi\hbar} \frac{\pi m}{16\hbar^2 q} \sum_n \int_0^\infty dE F_T(E - \mu) \{ \lambda_n(E) \tau_n^+(E) + \lambda_n(E - \hbar\omega) \tau_n^-(E - \hbar\omega) \}, \quad (10)$$

where

$$F_T(E - \mu) \equiv -\partial f^0(E) / \partial E = (1/4k_B T) \cosh^{-2}[(E - \mu)/2k_B T], \quad (11)$$

$$\tau_n^\pm(E) \equiv \theta(E - E_-) [\pm \theta(E + \hbar\omega - E_n^{\text{max}}) \theta(E_n^{\text{max}} - E) - 4\phi_n(E) \theta(E - E_n^{\text{max}}) \theta(E_n^{\text{max}} + E - E) \theta(-p_-)], \quad (12)$$

$$\phi_n(E) \equiv 1 + \sin[\varphi_n(E)],$$

$$\varphi_n(E) \equiv \frac{2}{\hbar} \int_0^{|x^*|} dx [\hbar q - |p(x; E)| - |p(x; E + \hbar\omega)|],$$

$$\lambda_n(E) \equiv \frac{V_0^2(x^*)}{E - E_-} \frac{d(x^*)}{|d'(x^*)|}, \quad (13)$$

$E_- = p_-^2/2m \equiv (mw - \hbar q/2)^2/2m$, $E_n^{\text{max}} \equiv E_n(0)$ is the maximum of the n th mode transverse energy, and the transition point $x^* = x^*(n, E)$ is given by $E_n(x^*) = E - E_-$. In this expression for G^{ac} , the θ functions involving E_- express the condition of the existence of a transition point x^* , the con-

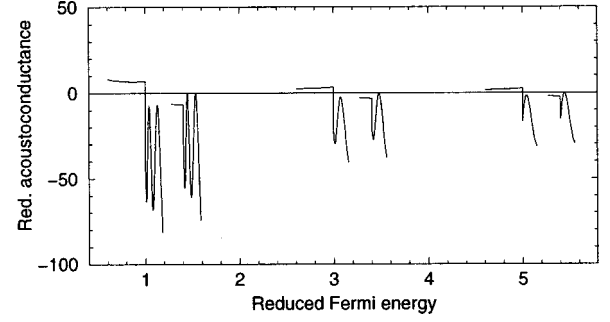


FIG. 5. Employing Eq. (10) for the case of an exponential channel geometry $d(x) = d \exp(x^2/2l^2)$ and a parabolic confining potential, the acoustoconductance G^{ac} is plotted [in units of $(2e^2/h) \times (V_0/E_0^{\text{max}})^2$, $E_0^{\text{max}} = \hbar^2/2md^2$ being the maximum of the zeroth mode transverse energy] as a function of the Fermi energy μ (in units of E_0^{max}). The figure shows the oscillations around the first 3 transverse energy maxima E_n^{max} ($n=0,1,2$). The sinelike curves have been cut at Fermi energies where the stationary phase approximation becomes unreasonable [i.e., we have required $|\sqrt{2}\varphi'''(x^*)/3\varphi''(x^*)^{3/2}| \leq 0.2$, cf. Ref. 36]. The parameters are $T=0$, $m=0.067 m_e$, $q=1.0 \times 10^5 \text{ cm}^{-1}$, $\omega=2.0 \times 10^{10} \text{ s}^{-1}$, $w=\omega/q=1.9 \times 10^5 \text{ cm/s}$, $l=5.0 \text{ }\mu\text{m}$, $d=0.13 \text{ }\mu\text{m}$; this gives $\hbar\omega=1.5 E_- \approx 0.4 E_0^{\text{max}}$. For simplicity, the envelope function $V_0(x)$ is assumed to be constant for the values of x^* involved in the computation.

stant factor $\theta(-p_-)$ tells whether backscattering processes are possible at all with the given wave parameters ω and q , while the other θ functions correspond to the conditions of propagation and reflection.

IV. DISCUSSION

Below we use some model parameters to illustrate the implications of Eq. (10). Figure 5 shows the dependence of the acoustoconductance G^{ac} on the Fermi energy μ for an exponential channel width $d(x) = d \exp(x^2/2l^2)$ and a parabolic confining potential leading to the Gaussian x dependence of the transverse energies,

$$E_n(x) = (2n+1)E_0^{\text{max}} \exp(-x^2/l^2), \quad E_0^{\text{max}} \equiv \hbar^2/2md^2.$$

The dimensions of the contact (l and d) are chosen such that the use of the stationary phase approximation is justified. Although the corresponding physical situation is realizable,³⁹ ballistic contacts that are normally used in experiments are smaller. Furthermore, the channel's width d exceeds the effective Bohr radius (cf. the discussion in Sec. II). This means that the envelope function $V_0(x)$ will in fact depend on y as well, due to strong screening inside the channel. Consequently, the oscillation pattern in Fig. 5 will actually be overlapped by contributions corresponding to nondiagonal transitions. However, in realistic situations (with narrow channels), those nondiagonal contributions do not occur. Therefore, the oscillatory behavior of the acoustoconductance, which is demonstrated by our model formula, should remain qualitatively right also in those situations.

With zero temperature (as in Fig. 5), the energies E in the above equations may be replaced by the Fermi energy μ . As the gate voltage is varied, the various energy-dependent θ functions begin or cease to give contributions to the acous-

toconductance G^{ac} . As a result, G^{ac} is nonzero only in regions where the Fermi energy is close to one of the transverse energy maxima E_n^{max} , that is, near gate voltages where the conductance makes a step.

In our approximation, there are two different kinds of ‘‘oscillations’’ in these regions. The first one involves an abrupt change of G^{ac} , which is due to the onset or offset of one or several θ functions. If we were dealing with wave parameters ω and q for which $p_- > 0$, then these steplike oscillations would be the only ones present. More specifically, for each transverse energy maximum E_n^{max} , the acoustoconductance would be positive and slowly varying in the region $E_n^{\text{max}} - \hbar\omega < \mu < E_n^{\text{max}}$, then negative and slowly varying in the following region $E_n^{\text{max}} < \mu < E_n^{\text{max}} + \hbar\omega$.

However, with the parameters used for Fig. 5, p_- is negative, i.e., $\hbar q > 2m\omega$. This means that backscattering processes are possible. Since there are two different transition points in these processes, the result is interference between the two reflected waves. Accordingly, there are additional, smooth oscillations of G^{ac} that clearly appear sinelike [cf. the function ϕ_n appearing in Eq. (12)].

To see which terms in the formula for the acoustoconductance contribute to the oscillations in the various Fermi level regions, consider as an example the oscillations near the zeroth mode energy maximum (i.e., where μ/E_0^{max} is close to 1). At first, in the region $E_0^{\text{max}} - \hbar\omega \approx 0.6 E_0^{\text{max}} < \mu < E_0^{\text{max}}$, the acoustoconductance is positive. This is just where the first term in Eq. (7) gives a (positive) contribution to G^{ac} . Above E_0^{max} , there are only negative terms. In the region $E_0^{\text{max}} < \mu < E_- \approx 1.3 E_0^{\text{max}}$, both the second and third terms are nonzero, the former diverging as μ approaches E_- . Only the third one is nonzero between E_- and $E_0^{\text{max}} + \hbar\omega \approx 1.4 E_0^{\text{max}}$. Finally, the fourth term is nonzero in the region $E_0^{\text{max}} + \hbar\omega < \mu < E_0^{\text{max}} + \hbar\omega + E_- \approx 1.7 E_0^{\text{max}}$, also eventually diverging. The second and fourth terms are the ones corresponding to interference and thus causing the sine-like oscillations.

ACKNOWLEDGMENTS

We are grateful to V. L. Gurevich for discussions. Two of the authors (H.T. and Ø.L.B.) are grateful to the Norwegian Research Council for financial support.

- ¹C. W. J. Beenakker and H. van Houten, in *Solid State Physics*, edited by H. Ehrenreich and D. Turnbull (Academic, San Diego, 1991), Vol. 44, p. 1.
- ²B. J. van Wees, H. van Houten, C. W. J. Beenakker, J. G. Williamson, L. P. Kouwenhoven, D. van der Marel, and C. T. Foxon, *Phys. Rev. Lett.* **60**, 848 (1988).
- ³D. A. Wharam, T. J. Thornton, R. Newbury, M. Pepper, H. Ahmed, J. E. F. Frost, D. G. Hasko, D. C. Peacock, D. A. Ritchie, and G. A. C. Jones, *J. Phys. C* **21**, L209 (1988).
- ⁴R. Landauer, *IBM J. Res. Dev.* **1**, 233 (1957); **32**, 306 (1989).
- ⁵I. O. Kulik, R. I. Shekhter, and A. N. Omelyanchouk, *Solid State Commun.* **23**, 301 (1977).
- ⁶V. L. Gurevich, V. B. Pevzner, and G. Iafrate, *Phys. Rev. Lett.* **75**, 1352 (1995).
- ⁷A. Grincwajg, L. Y. Gorelik, V. Z. Kleiner, and R. I. Shekhter, *Phys. Rev. B* **52**, 12 168 (1995).
- ⁸H. Karl, W. Dietsche, A. Fischer, and K. Ploog, *Phys. Rev. Lett.* **61**, 2360 (1988).
- ⁹L. J. Challis, A. J. Kent, and V. W. Rampton, *Semicond. Sci. Technol.* **5**, 1179 (1990).
- ¹⁰A. J. Kent, *Physica B* **169**, 356 (1991).
- ¹¹D. J. McKitterick, A. Shik, A. J. Kent, and M. Henini, *Phys. Rev. B* **49**, 2585 (1994).
- ¹²A. J. Naylor, K. R. Strickland, A. J. Kent, and M. Henini, *Surf. Sci.* **361/362**, 660 (1996).
- ¹³A. J. Kent, A. J. Naylor, P. Hawker, M. Henini, and B. Bracher, *Phys. Rev. B* **55**, 9775 (1997).
- ¹⁴M. Blencowe and A. Shik, *Phys. Rev. B* **54**, 13 899 (1996).
- ¹⁵A. Wixforth, J. P. Kotthaus, and G. Weimann, *Phys. Rev. Lett.* **56**, 2104 (1986).
- ¹⁶A. Wixforth, J. Scriba, M. Wassermeier, J. P. Kotthaus, G. Weimann, and W. Schlapp, *Phys. Rev. B* **40**, 7874 (1989).
- ¹⁷R. L. Willett, M. A. Paalanen, R. R. Ruel, K. W. West, L. N. Pfeiffer, and D. J. Bishop, *Phys. Rev. Lett.* **65**, 112 (1990).
- ¹⁸R. L. Willett, R. R. Ruel, M. A. Paalanen, K. W. West, and L. N. Pfeiffer, *Phys. Rev. B* **47**, 7344 (1993).
- ¹⁹R. L. Willett, R. R. Ruel, K. W. West, and L. N. Pfeiffer, *Phys. Rev. Lett.* **71**, 3846 (1993).
- ²⁰C. Rodrigues, A. L. A. Fonseca, and O. A. C. Nunes, *Phys. Status Solidi B* **189**, 117 (1995).
- ²¹G. R. Nash, S. J. Bending, Y. Kershaw, K. Eberl, P. Grambow, and K. von Klitzing, *Surf. Sci.* **361/362**, 668 (1996).
- ²²A. L. Efros and Yu. M. Galperin, *Phys. Rev. Lett.* **64**, 1959 (1990).
- ²³A. Esslinger, A. Wixforth, R. W. Winkler, J. P. Kotthaus, H. Nickel, W. Schlapp, and R. Löscher, *Solid State Commun.* **84**, 939 (1992).
- ²⁴V. I. Fal’ko, S. V. Meshkov, and S. V. Iordanskii, *Phys. Rev. B* **47**, 9910 (1993).
- ²⁵J. M. Shilton, D. R. Mace, V. I. Talyanskii, M. Pepper, M. Y. Simmons, A. C. Churchill, and D. A. Ritchie, *Phys. Rev. B* **51**, 14 770 (1995).
- ²⁶J. M. Shilton, D. R. Mace, V. I. Talyanskii, M. Y. Simmons, M. Pepper, A. C. Churchill, and D. A. Ritchie, *J. Phys.: Condens. Matter* **7**, 7675 (1995).
- ²⁷J. M. Shilton, D. R. Mace, V. I. Talyanskii, Yu. Galperin, M. Y. Simmons, M. Pepper, and D. A. Ritchie, *J. Phys. Condens. Matter* **8**, L337 (1996).
- ²⁸J. M. Shilton, V. I. Talyanskii, M. Pepper, D. A. Ritchie, J. E. F. Frost, C. J. B. Ford, C. G. Smith, and G. A. C. Jones, *J. Phys. Condens. Matter* **8**, L531 (1996).
- ²⁹H. Totland and Yu. Galperin, *Phys. Rev. B* **54**, 8814 (1996).
- ³⁰V. L. Gurevich, V. G. Skobov, and Yu. A. Firsov, *Zh. Éksp. Teor. Fiz.* **40**, 786 (1961) [*Sov. Phys. JETP* **13**, 552 (1961)].
- ³¹V. L. Gurevich, V. B. Pevzner, and G. J. Iafrate, *Phys. Rev. Lett.* **77**, 3881 (1996).
- ³²F. A. Maaß and Yu. M. Galperin, *Phys. Rev. B* **56**, 4028 (1997).
- ³³L. D. Landau and E. M. Lifshitz, *Quantum Mechanics*, 3rd ed. (Pergamon, Oxford, 1977), Chap. 7.
- ³⁴S. H. Simon, *Phys. Rev. B* **54**, 13 878 (1996).

- ³⁵A. Knäbchen, Y. B. Levinson, and O. Entin-Wohlman, *Phys. Rev. B* **55**, 5325 (1997).
- ³⁶One condition for the expansion (3) to be valid is $|\varphi'''(x^*)/\varphi''(x^*)^{3/2}| \ll 1$. However, the quantity on the lhs diverges as x^* approaches 0. Furthermore, $\frac{1}{2}|\varphi''(x^*)|x^{*2}$ should be greater than 1.
- ³⁷The wave function of a nonpropagating state $|n, p\rangle$ is proportional to $\exp(ip dx') - \exp(-ip dx')$, and hence there are two integrands in the transition amplitude (if the other state is a propagating one). At most one of the corresponding phases has a stationary point, and only that part of the integral will be kept in the calculations.
- ³⁸The geometrical representation of complex numbers and their operations was first introduced in 1797 by C. Wessel in a thesis to the Royal Danish Academy of Sciences and Letters (translated version to be published).
- ³⁹S. Datta, *Electronic Transport in Mesoscopic Systems* (Cambridge University Press, Cambridge, 1995), p. 2.